Electrochimica Acta 70 (2012) 118–123

Contents lists available at SciVerse ScienceDirect

Electrochimica Acta

journal homepage: www.elsevier.com/locate/electacta

XRD, SEM and photoelectrochemical characterization of ZnSe electrodeposited on Cu and Cu–Sn substrates

Remigijus Juškėnas*,[1], Darius Avižinis, Putinas Kalinauskas, Algirdas Selskis[1], Raimondas Giraitis, Vidas Pakštas, Violeta Karpavičienė, Stasė Kanapeckaitė, Zenius Mockus, Rokas Kondrotas

State Research Institute Center for Physical Sciences and Technology, Institute of Chemistry, A. Goštauto 9, LT-01108 Vilnius, Lithuania

ARTICLE INFO

Article history:
Received 2 December 2011
Received in revised form 10 March 2012
Accepted 10 March 2012
Available online 27 March 2012

Keywords:
Electrodeposition
Zinc selenide
Photoelectrochemical response
XRD

ABSTRACT

XRD, SEM and photoelectrochemical examinations of deposits formed on the Cu substrate by electrochemical deposition in a water solution containing 0.2 mol dm^{-3} of $ZnSO_4$ and 0.002 mol dm^{-3} of H_2SeO_3 were performed. Formation of Cu_2Se_x at potentials positive to that of electrochemical deposition of ZnSe was proved by the XRD technique. The formation of Cu_2Se_x continued even after deposition due to further diffusion of the deposited Se into Cu. A nano-crystalline ZnSe of cubic structure was electrodeposited at a potential of −0.62 V vs. Ag/AgCl electrode and XRD examination of deposits formed using cyclic potential scanning and pulse plating revealed the presence of hexagonal ZnSe along with the cubic one. A photoelectrochemical characterization proved that the electrodeposited ZnSe was a p-type semiconductor. A significant amount of Cu_2Se_x was formed during annealing of ZnSe electrodeposited on the Cu substrate although only traces of copper selenide were detected before the annealing. ZnSe, SnSe and a small quantity of Cu_2Se_x were detected by XRD after annealing of ZnSe electrodeposited on the Cu–Sn/Mo/glass substrate.

1. Introduction

ZnSe is an n-type semiconductor with a wide band gap (2.7 eV) and has a lot of technological applications. The electrodeposition of ZnSe has been intensively investigated during past 30 years. One of the most promising appliances of the electrodeposited ZnSe could be fabrication of the CZTSe ($Cu_2ZnSnSe_4$) absorber layer for thin film solar cells [1,2]. Instead of electrodeposition of stacked layers of Cu, Sn and Zn, ZnSe could be deposited on a Cu–Sn layer. The electrodeposition of ZnSe instead of Zn can make it possible to avoid an insertion of $Zn(OH)_2$/ZnO into the deposit which usually takes place when cyanide-free solutions are used for the electrodeposition of Zn or Zn alloys [3,4].

The electrodeposition of ZnSe has been investigated mainly in water solutions [5–16] though in organic ones it has also been reported [17]. In general zinc sulphate aqueous solutions to which a small quantity of Se is added in the form of H_2SeO_3 or SeO_2 are used [5–10,12,13]. Different solutions such as acetate [13], perchlorate [15], and solutions containing zinc EDTA (ethylene diamine tetraacetate) complex and selenium sulphite [8] have been examined. The electrodeposition of ZnSe was carried out on different substrates such as Ti [5–10,12], glass coated with ITO (indium doped tin oxide) or FTO (fluorine doped tin oxide) [5–9,11,17], stainless steel (SS) [11,12], Au [5,15], Cu [13,14]. The electrodeposited ZnSe is predominantly reported to have a cubic structure except when it was electrodeposited on the SS or Al substrates on which ZnSe possessed a hexagonal structure [12]. It has been reported that electrodeposited zinc selenide was a p-type semiconductor [5].

The electrodeposition of ZnSe on the Cu substrate was comprehensively studied by Kowalik et al. [13,14]. The electrolyte solution containing 0.2 mol dm^{-3} $ZnSO_4$ and 0.002 mol dm^{-3} H_2SeO_3 was determined as the most suitable one for electrodeposition of ZnSe, the most preferable potential and solution temperature ranges were also established [13].

When considering a possibility to use the electrodeposition of ZnSe for the electrochemical approach of the CZTSe fabrication it could be useful to conduct more detailed studies of ZnSe deposition on the copper substrate as one of the possible routes of the electrochemical formation of copper selenide can proceed through the reaction proposed by Kazacos and Miller [16]:

$$2Cu + H_2SeO_3 + 4e^- + 4H^+ \rightarrow Cu_2Se + 3H_2O \quad (1)$$

However, as yet it has not been evidenced by XRD the Cu_2Se is formed during the electrochemical ZnSe deposition on the Cu substrate. It has been reported that only amorphous selenium was detected on the Cu substrate when the electrochemical deposition was carried out in the potential range from 0 to −0.5 V vs. SCE

* Corresponding author. Tel.: +370 5 264 8881; fax: +370 5 264 9774.
E-mail address: juskenas@ktl.mii.lt (R. Juškėnas).
[1] ISE member.

0013-4686/$ – see front matter © 2012 Elsevier Ltd. All rights reserved.
http://dx.doi.org/10.1016/j.electacta.2012.03.103

[13,14]. Even after 2 h of heat treatment of the electrodeposited ZnSe on Cu in Ar atmosphere at 300 °C formation of copper selenide was not detected by XRD [13]. Nevertheless, on the basis of the data obtained using voltammetry combined with the quartz crystal microbalance technique the assumption was made that the electrodeposited Se interacts with Cu at least during the first cycle of electrodeposition [14].

In this work we present electrochemical, XRD, SEM along with EDX and photoelectrochemical investigations of electrodeposits formed on the Cu substrate in aqueous zinc sulphate solutions with selenious acid. We used a combined electrochemical striping/XRD approach [4,18] while attempting to get more information about the crystalline phases formed. We also applied heat treatment of electrodeposited coatings to learn more about the nano-crystalline or amorphous phases formed. By the mentioned means we succeeded to detect two modifications of zinc selenide and one modification of copper selenide formed on the copper substrate along with amorphous elemental selenium during the electrodeposition of ZnSe.

2. Experimental

The electrodeposition was carried out (1) potentiostatically, (2) applying cyclic potential scanning in an appropriate potential range (3) using pulses of different potential and duration. Parameters of the two latter approaches will be indicated when presenting the results obtained. A potentiostat PI-50-1.1 connected with PC was used for control and data acquisition.

An electrolyte solution of optimal composition (0.2 mol dm^{-3} $ZnSO_4$ and 0.002 mol dm^{-3} H_2SeO_3 [13]) was prepared using triply-distilled water and analytical grade reagents. The pH of the solution was adjusted to 2.0 using H_2SO_4 and a temperature of +30 ± 0.5 °C was maintained. A three-compartment glass electrolytic cell was used. A copper foil of 1 × 1 cm^2 geometrical area was used as a working electrode, which prior to electrodeposition was chemically etched in a 1:1:1 volume ratio mixture of acids: HNO_3, H_3PO_4, CH_3COOH and next rinsed with a stream of triply-distilled water. A Cu–Sn layer on Mo was electrodeposited in a citrate solution containing 0.02 mol dm^{-3} $CuSO_4$ and 0.01 mol dm^{-3} $SnSO_4$. A Pt (purity 99.995) plate of 1.5 × 2 cm^2 geometrical area was used as a counter electrode. Ag/AgCl/KCl (saturated) was used as a reference electrode and all potentials are given versus this electrode. The electrolyte solution was purged by Ar 5.0 gas for 1 h prior to electrodeposition and it was kept purging during the deposition.

A phase composition of the deposits was examined by an X-ray diffractometer D8 Advance (Bruker AXS) with Cu K_α radiation (λ = 1.54183 Å, U_a = 40 kV, I_a = 40 mA) separated by a curved multilayer monochromator mounted on the primary beam. Symmetrical $\Theta/2\Theta$ geometry and grazing incidence (GIXRD) techniques were used and in the latter case the incidence angle (Θ angle) was 0.5°. The XRD patterns were measured in 2Θ range from 10 to 60° in a step scan mode: a step size ($\Delta 2\Theta$) 0.04°, counting duration 5 s.

The surface morphology and chemical composition were examined by a scanning electron microscope Helios Nanolab 650 (FEI company) with EDX (Oxford instruments).

The photoelectrochemical response was measured in a home-made cell in a 0.2 mol dm^{-3} aqueous solution of K_2SO_4. The measurement technique is presented elsewhere [19].

3. Results and discussions

Cyclic voltammograms shown in Fig. 1 have the same characteristic cathodic and anodic peaks which have been reported by other

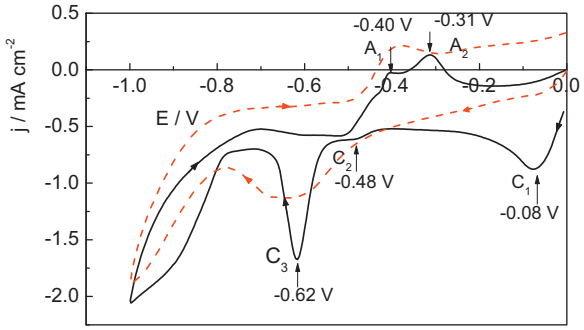

Fig. 1. Cyclic voltammogram for Cu electrode in solution (mol dm^{-3}): 0.2 $ZnSO_4$, 0.002 H_2SeO_3, pH 2.0, T = +30 °C. Potential scan rate 20 mV s^{-1}.

authors [13,14]. The most positive cathodic peak is attributable to the electrodeposition of Se according to the equation:

$$H_2SeO_3 + 4H^+ + 4e^- = Se + 3H_2O \quad (2)$$

However, Eq. (1) mentioned in the Introduction section should be taken into account. A shift of cathodic peak C_1 to positive potentials during further cycling reported by Kowalik and Fitzner [14] could be caused by the formation of Cu_2Se during the first cycle.

To verify if reaction (1) takes place potentiostatic deposition was carried out at potential C_1 during 60 min and the XRD pattern of the deposit obtained was measured immediately after the deposition. The XRD pattern (Fig. 2) proves copper selenide to be formed during Se electrodeposition on the copper substrate. Nearly all the XRD peaks on the pattern match fairly well with those presented in PDF file no. 47-1448 for orthorhombic Cu_2Se_x. No peaks attributable to elemental Se can be seen on the pattern. Nevertheless it could be supposed that some amount of elemental selenium was present in an amorphous state.

The quantity of Cu_2Se_x increased with electrodeposition time. Fig. 3 presents a ratio of integral intensity of XRD peak of Cu_2Se_x at $2\Theta \approx 51.9°$ to that of Cu 200 as a function of the deposition time. An increasing quantity of the Cu_2Se_x with deposition time could mean that rather fast diffusion of Se into Cu takes places even at a temperature of +30 °C. The ratio increased yet more 3 days after deposition for samples deposited during 20 and 40 min though it remained constant for that deposited during 60 min. That could be caused by further diffusion of the deposited amorphous selenium into the copper substrate even when the deposition has finished. It is in agreement with the results of other researchers and proves that amorphous selenium diffuses into copper [20]. However, there is a certain limit of the diffusion depth as for the sample

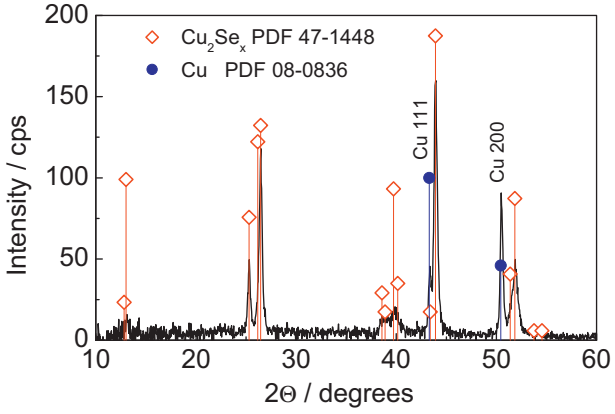

Fig. 2. XRD pattern for the deposit obtained on the Cu cathode at potential of C_1 (−0.08 V vs. Ag/AgCl).

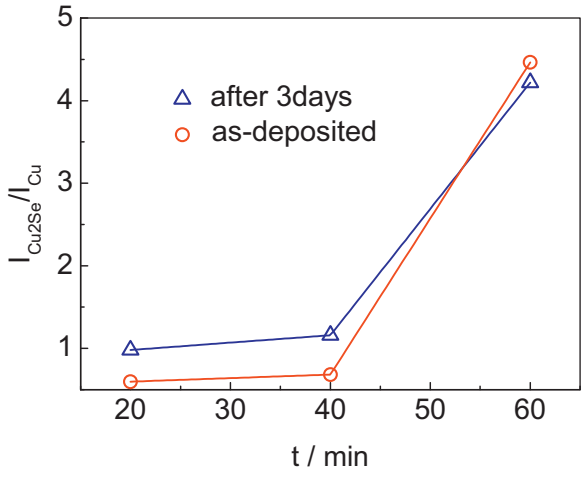

Fig. 3. Ratio of intensity of the XRD peak Cu_2Se_x at 2Θ of 51.9° to that of Cu 200 as a function of deposition time.

deposited during 60 min the intensity ratio does not significantly change with the aging time.

The above presented assumptions can get one more evidence if compare the ratio of the integral intensity of XRD peak of Cu_2Se_x at $2\Theta \approx 51.9°$ measured by GIXRD to that obtained using $\Theta/2\Theta$ geometry (Fig. 4). The first intensity depicts the quantity of Cu_2Se_x at the surface of Cu electrode and the second one in the bulk of it. The ratio decreases with deposition time indicating that the layer of Cu_2Se_x becomes thicker. The thickness of the layer increases also with the aging time.

The XRD patterns for the deposits obtained at more negative potentials (−0.2 and −0.4 V) look quite similar to that shown in Fig. 2.

Fig. 5 shows the XRD pattern for the coating electrodeposited at the potential of cathodic peak C_2 (−0.48 V) during 60 min. Three broad and two narrow XRD peaks are seen on the pattern. The broad ones match well with those presented in PDF no. 37-1463 for cubic ZnSe and the narrow ones correspond to copper (PDF no. 04-0836). Such broad XRD peaks of ZnSe are indicative of a nanostructured material. The crystallite size of ZnSe in crystallographic direction ⟨1 1 1⟩ was calculated using Scherrer equation and was equal to 3.7 ± 0.8 nm. The increase in quantity of selenious acid in the electrolyte solution up to 0.01 mol dm^{-3} shifts the potential of cathodic peak C_2 to a more negative potential −0.52 V and it results in an increase in the quantity of electrodeposited ZnSe.

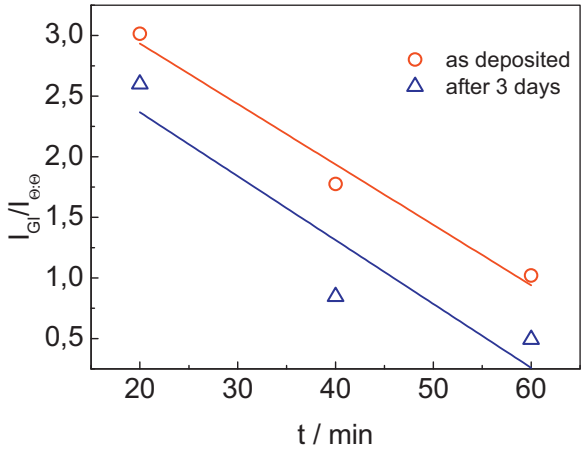

Fig. 4. Ratio of intensity of the XRD peak Cu_2Se_x at 2Θ of 51.9° measured in the GIXRD geometry to that obtained in $\Theta/2\Theta$ one as a function of deposition time.

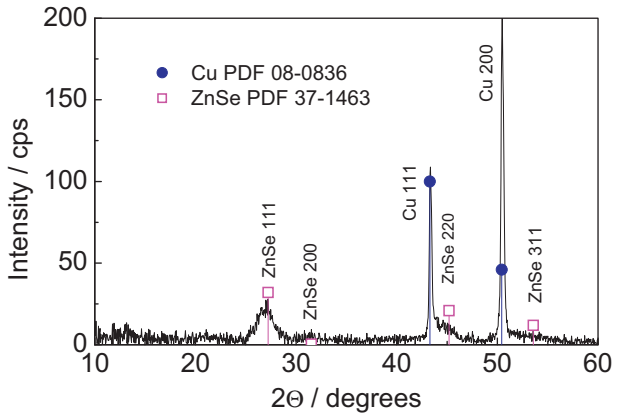

Fig. 5. XRD pattern for the deposit obtained on the Cu cathode at potential of C_2 (−0.48 V vs. Ag/AgCl).

Fig. 6 presents the XRD pattern (black solid curve) for deposit obtained at the potential of cathodic peak C_3 (−0.62 V) during 60 min. The pattern looks close to that of the coating electrodeposited at the potential of −0.48 V, however the XRD peaks of ZnSe are of higher intensity. The ZnSe is obviously nano-crystalline. An appropriate procedure of recrystallization can significantly improve the crystallinity of a nano-crystalline material and, consequently, the quality of XRD pattern. Fig. 6 presents the XRD pattern (red thin curve) for the same deposit after annealing at +300 °C in Ar atmosphere for 3 h. Very sharp XRD peaks appeared on the pattern of the annealed sample and they apparently corresponded to cubic ZnSe, orthorhombic Cu_2Se_x and Cu. A small amount of ZnO (PDF no. 36-1451) was also present. The results obtained can be explained assuming that at a potential of −0.62 V along with formation of ZnSe the electrodeposition of Se and insertion of amorphous $Zn(OH)_2$ took place. While annealing the latter two phases were transformed into Cu_2Se_x and ZnO, respectively. The presence of Se phase in the as-deposited ZnSe coating was confirmed by EDX: the quantity of Se was higher by 8–15 at.% compared with that of Zn in the deposit (Table 1).

SEM images of deposits electrochemically formed on the Cu electrode at different potentials (E = −0.08 V, left-side images, and E = −0.62 V, right-side images) are shown in Fig. 7. The deposit obtained at E = −0.08 V presents disk-like agglomerates of Cu_2Se_x crystallites according to XRD data (Fig. 2). Most of the disks are perpendicular to the electrode surface. Results of EDX measurements of the deposits are shown in Table 1. No zinc was detected in

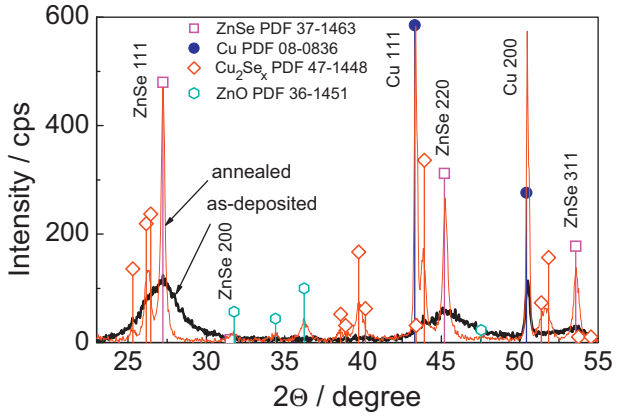

Fig. 6. XRD pattern for the deposit formed on the Cu cathode at potential of C_3 (−0.62 V vs. Ag/AgCl). (For interpretation of the reference to color in the text for Fig. 6, the reader is referred to the web version of the article.)

Table 1
Chemical composition of deposits electrochemically formed on Cu cathode in solution containing 0.2 mol dm^{-3} of $ZnSO_4$ and 0.002 mol dm^{-3} of H_2SeO_3.

E (V)	Examined area notation	Cu (at.%)	Se (at.%)	Zn (at.%)
−0.08	1	72.2 ± 4.5	27.8 ± 4.5	–
−0.08	2	78.6 ± 4.5	21.4 ± 4.5	–
−0.62	3	51.7 ± 2.5	27.8 ± 2.5	20.5 ± 3.3
−0.62	4	53.9 ± 2.5	29.0 ± 2.5	17.1 ± 3.3
−0.62	5	37.1 ± 2.5	39.3 ± 2.5	23.6 ± 3.3

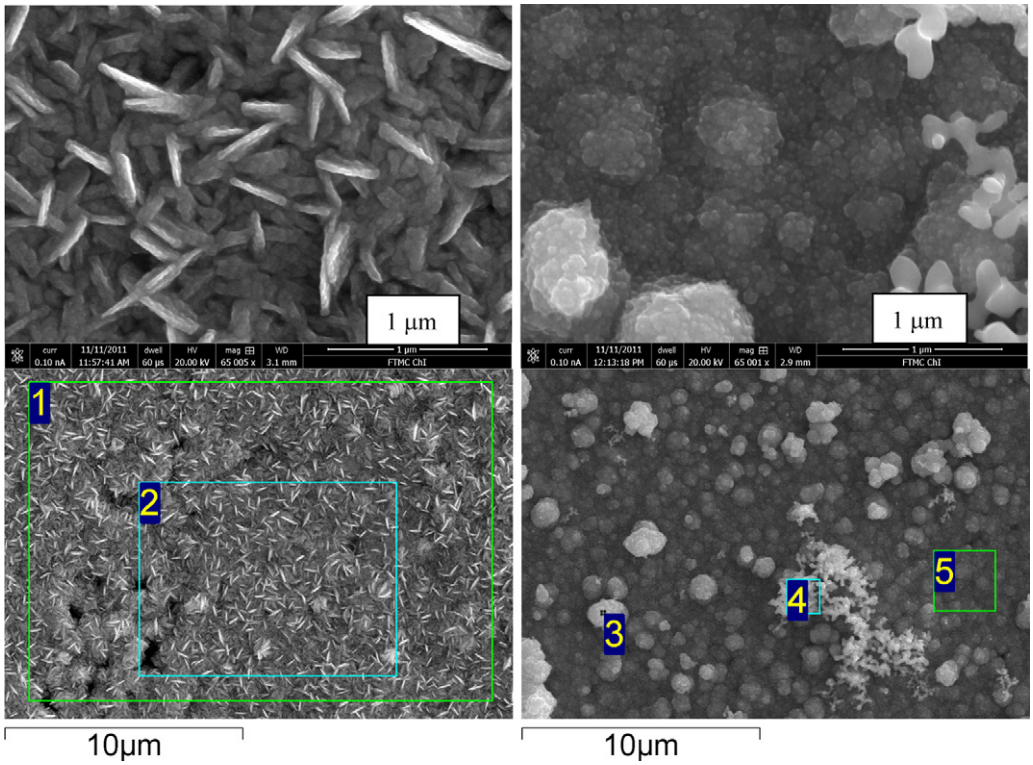

Fig. 7. SEM images of deposits formed at potential of C_1 (left-side images) and of C_3 (right-side images).

the deposits obtained at $E = -0.08$ V. The quantity of Se measured from a larger area (assigned "1" on left-side lower image, Fig. 7) was slightly lower since this area contains more dark spots which could be holes in the deposit layer. The deposit of ZnSe (right side images, Fig. 7) mostly presents globular agglomerates of ZnSe crystallites whose size should be 3–5 nm according to the broad XRD peaks of ZnSe (Fig. 6). Bright particles (assigned "3" and "4" on the right-side lower image, Fig. 7) emerging on the top of darker globular agglomerates (assigned "5" on right-side lower image, Fig. 7) contains a larger quantity of Se (Table 1). These particles could be crystalline selenium, however it was not confirmed by XRD due to a small quantity of these particles.

In attempt to discover the origin of anodic peaks A_1 and A_2 (Fig. 1) electrodeposition was carried out using cyclic potential scanning forwards and backwards in the potential range from −0.4 to −0.62 V, i.e. from the potential of anodic peak A_1 to that of cathodic C_3. It was suggested that such deposition should yield a relative increase in the quantity of the substance which electrochemically dissolves at the potential of anodic peak A_2 [4,18]. The cycling with a potential scan rate of 10 mV s^{-1} proceeded for 60 min. Fig. 8 shows an XRD pattern of the coating electrodeposited using the above described approach. It can be clearly seen that the XRD peak ZnSe 1 1 1 became sharper if compared with that in Fig. 6 (FWHM equaled 1.1° and 2.6°, respectively) and small knolls appeared on the both shoulders of this peak (marked with "?" symbols on Fig. 8). These features could indicate that at the anodic potential of A_1 the nano-crystalline fraction of cubic ZnSe was dissolved making the XRD peak ZnSe 1 1 1 sharper and small peaks of some other phase more distinct.

It could be supposed that the phase, which became detectable in Fig. 8 (upper red curve) should dissolve at a more positive potential of anodic peak A_2. So the same cyclic potential scanning approach

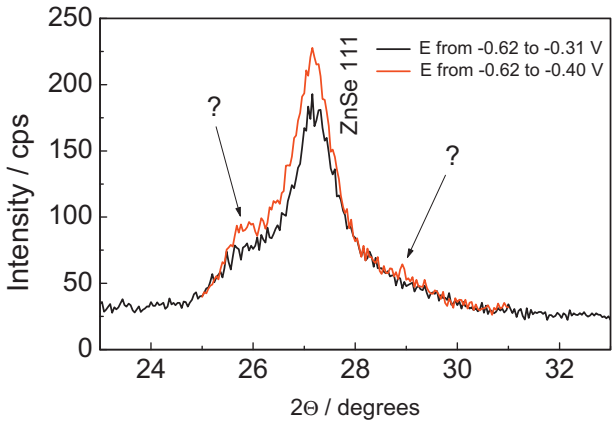

Fig. 8. XRD pattern for the deposit formed on the Cu cathode by cyclic potential scanning. The potential scan rate 10 mV s^{-1}.

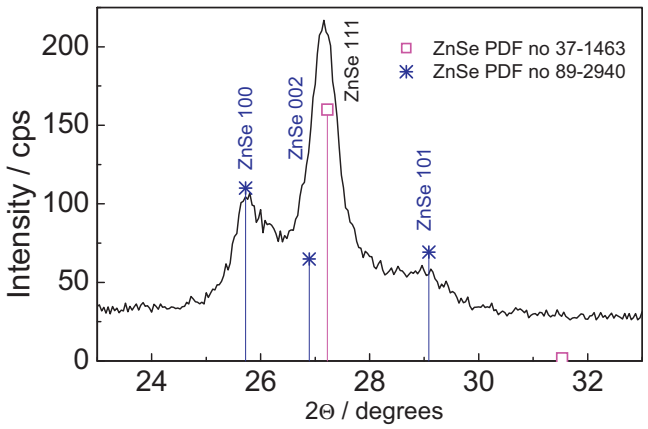

Fig. 9. XRD pattern for the deposit formed on the Cu cathode by pulse electrodeposition: $E_1 = -0.62$ V, $t = 10$ s; $E_2 = -0.31$ V, $t = 8$ s.

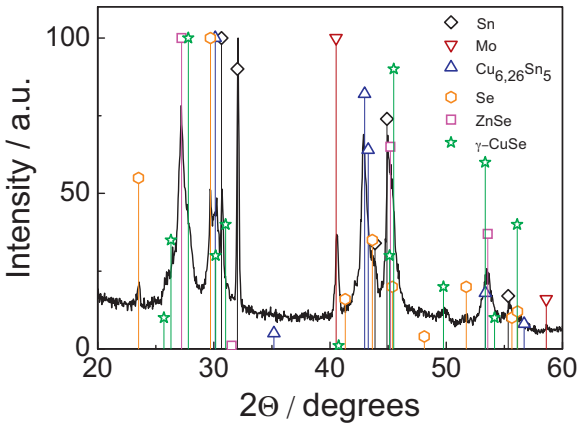

Fig. 11. XRD pattern for the ZnSe deposit formed on the Cu–Sn cathode. Sn – PDF no. 04-0673; Mo – PDF no. 42-1120; $Cu_{6,26}Sn_5$ – PDF no. 47-1575; Se – PDF no. 06-0362; ZnSe – PDF no. 37-1463; γ-CuSe – PDF no. 27-0185.

was employed for the potential range from −0.31 to −0.62 V. The ZnSe peaks remained sharp as in the previous case and the knolls on the shoulders of XRD peak ZnSe 1 1 1 became less visible, especially the one on the right shoulder (Fig. 8, lower black curve). It could be inferred that the assumption regarding dissolution of the unknown phase was confirmed.

According to Kowalik et al. [13] anodic peak A_2 could be related to the process of desorption of species adsorbed during potential scan in the cathodic direction. To reduce quantity of the adsorbed species, a pulse electrodeposition was tried in attempt to find out the origin of the unknown phase. Short pulses of two potentials were repeatedly used for 60 min. The first pulse was at potential $E_1 = -0.62$ V, with duration $t = 10$ s and the second one at that of −0.31 V, $t = 8$ s. Fig. 9 shows an XRD pattern of the coating electrodeposited using the above described approach. Two distinct peaks appeared on the both sides of XRD peak ZnSe 111 and they are attributable to the hexagonal ZnSe phase (PDF no. 89-2940). The result obtained infers that usage of short pulses make it possible to more effectively remove the adsorbed species which results in formation of ZnSe of a better crystallinity.

The photoelectrochemical response of ZnSe electrodeposited at a potential of −0.62 V is shown in Fig. 10. The response of electrochemical system to the optical perturbation was investigated by recording the dynamics of the photopotential under open-circuit conditions. Light diodes emitting light of different wavelength (indicated in Fig. 10) were used in sequence to illuminate the ZnSe surface and the open-circuit potential corresponding to different wavelength was measured. The potential difference for dark and illuminated ZnSe was 3–5 mV only until the light wavelength was ≥530 nm. For the wavelength of 505 nm the difference of open-circuit potential reached +20 mV and for that of 455 nm +38 mV indicating that the ZnSe deposit was a p-type semiconductor with a band-gap of about 2.5–2.7 eV.

As the first attempt to use the electrodeposition of ZnSe for fabrication of $Cu_2ZnSnSe_4$ for a thin film solar cell ZnSe was deposited on the electrodeposited Cu–Sn coating, which contained 65 at.% of Cu and 35 at.% of Sn according to EDX data. The cyclic voltammogram for the Cu–Sn electrode is shown in Fig. 1 (dashed curve). It was slightly different from that for the Cu electrode: there was no cathodic peak C_1 and the peak C_3 was broader. According to Kowalik and Fitzner [14] the cathodic peak C_1 is related to the interaction between selenium and copper during the deposition process. In the case of the Cu–Sn substrate copper selenide most probably did not form since the substrate did not contain a pure Cu phase (Fig. 11). On the other hand, it was shown by Lukinskas et al. [21] that the interaction of Se with Sn is very slow at room temperature. When electrodeposition of Se proceeded only according to reaction (2) a layer of grey electro-inactive Se was forming [14]. Those could be the reasons due to which a slow increase in cathodic current was seen instead of the peak C_1 in the cyclic voltammogram when the Cu–Sn substrate was used.

Fig. 11 shows the XRD pattern of as-deposited ZnSe on the layer of Cu–Sn electrodeposited on the Mo coated glass substrate. Along with peaks of $Cu_{6.25}Sn_5$ (PDF no. 47-1575), Sn (PDF no. 06-0362)

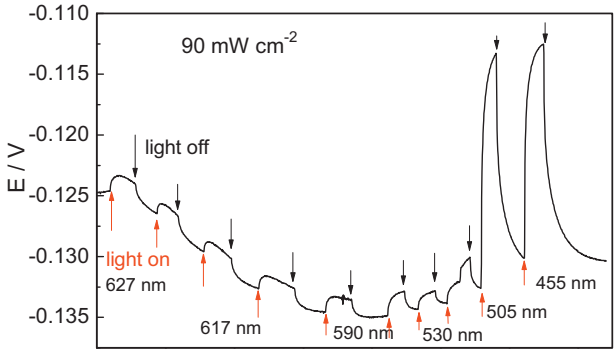

Fig. 10. Dependence of open circuit potential of the electrodeposited ZnSe on the wavelength of the illumination.

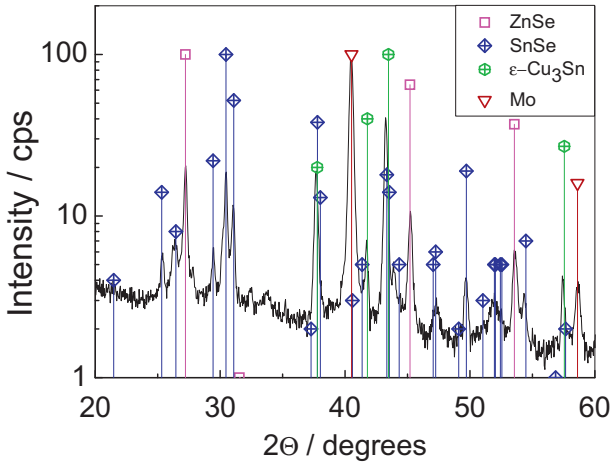

Fig. 12. XRD pattern for the ZnSe electrodeposited on the Cu–Sn cathode and annealed for 0.5 h in Ar atmosphere at +500 °C. SnSe – PDF no. 48-1224; ε-Cu_3Sn PDF no. 01-1240.

and Mo (PDF no. 42-1120) quite distinct peaks of ZnSe and Se (PDF no. 06-0362) are present. The presence of Cu_2Se is not apparent: only a broad peak at 2Θ of ~13° (not shown in Fig. 11) and a hump on the left side of peak ZnSe 1 1 1 could indicate the presence of it. Some peaks are attributable to γ-CuSe (PDF no. 27-0185).

Fig. 12 presents the XRD pattern of the previous sample after annealing at +500 °C in Ar atmosphere for 0.5 h. The pattern proves that SnSe (PDF no. 48-1224) was formed during the annealing. It is obvious that the quantity of Se in the deposit was insufficient to transform all the copper and tin into selenides since XRD peaks of ε-Cu_3Sn (PDF no. 01-1240) were well seen. Though $Cu_2ZnSnSe_4$ was not formed in the current experiment it can be supposed that kesterite is formed when annealing is carried out in Se or H_2Se atmosphere. And while using S or H_2S atmosphere during annealing a mixed S–Se kesterite with even better photovoltaic characteristics can be formed.

4. Conclusions

The XRD investigations of deposits electrochemically formed on the Cu substrate in the solution containing $ZnSO_4$ and H_2SeO_3 proved that copper selenide Cu_2Se_x is formed during the electrochemical process and even after it was ended. At the potential of electrochemical deposition of ZnSe the formation of Cu_2Se_x takes place as well, however to a much lesser extent. A nano-crystalline ZnSe of cubic structure was electrodeposited at a potential of −0.62 V and XRD examination of deposits formed using cyclic potential scanning and pulse plating revealed the presence of hexagonal ZnSe along with the cubic one. A photoelectrochemical characterization proved that the electrodeposited ZnSe was a p-type semiconductor. The formation of Cu_2Se_x in these deposits on the Cu substrate can be promoted by heating. The heat treatment of ZnSe deposits on the Cu–Sn layer resulted in formation of SnSe and Cu_2Se. The quantity of Se in ZnSe deposits was insufficient for the formation of $Cu_2ZnSnSe_4$.

Acknowledgment

This research was funded by a grant (no. ATE-07/2010) from the Research Council of Lithuania.

References

[1] S.G. Babu, K.Y.B. Kumar, U.P. Bhaskar, S. Raja Vanjari, Sol. Energy Mater. Sol. Cells 94 (2010) 221–226.
[2] P.M.P. Salome, J. Malaquias, P.A. Fernandes, M.S. Ferreira, J.P. Leitao, A.F. daCunha, J.C. Gonzalez, F.N. Matinaga, G.M. Ribeiro, E.R. Viana, Sol. Energy Mater. Sol. Cells 95 (2011) 3482–3489.
[3] T. Vagramyan, J.S.L. Leach, J.R. Moon, Electrochim. Acta 24 (1979) 231–236.
[4] R. Juškėnas, V. Karpavičienė, V. Pakštas, A. Selskis, V. Kapočius, J. Electroanal. Chem. 602 (2007) 237–244.
[5] G. Riveros, H. Gomez, R. Henriquez, R. Schrebler, R.E. Marotti, E.A. Dalchiele., Sol. Energy Mater. Sol. Cells 70 (2001) 255–268.
[6] S. Soundeswaran, O. Senthil Kumar, R. Dhanasekaran, P. Ramasamy, R. Kumaresen, M. Ichimura, Mater. Chem. Phys. 82 (2003) 268–272.
[7] S. Soundeswaran, O. Senthil Kumar, R. Dhanasekaran, P. Ramasamy, R. Kumaresen, M. Ichimura, Growth of ZnSe thin films by electrocrystallization technique, Mater. Chem. Phys. 82 (2003) 268–272.
[8] G. Riveros, D. Lincot, J.F. Guillemoles, R. Henriquez, R. Schrebler, R. Cordova, H. Gomez, J. Electroanal. Chem. 558 (2003) 9–17.
[9] T. Kosanovic, M. Bouroushian, N. Spyrelis, Mater. Chem. Phys. 90 (2005) 148–154.
[10] K.R. Murali, M. Balasubramanian, Mater. Sci. Eng. A 431 (2006) 118–122.
[11] Y.G. Gudage, N.G. Deshpande, A.A. Sagade, R. Sharma, J. Alloys Compd. 488 (2009) 157–162.
[12] A. Moses Ezhil Raj, S. Mary Delphine, C. Sanjeeviraja, M. Jayachandran, Physica B: Condens. Matter 402 (2010) 2485–2491.
[13] R. Kowalik, P. Žabinski, K. Fitzner, Electrochim. Acta 53 (2008) 6184–6190.
[14] R. Kowalik, K. Fitzner, J. Electroanal. Chem. 633 (2009) 78–84.
[15] A. Manzoli, M.C. Santos, S.A.S. Machado, Thin Solid Films 515 (2007) 6860–6866.
[16] M.S. Kazacos, B. Miller, J. Electrochem. Soc. 127 (1980) 869–873.
[17] R. Henriquez, H. Gomez, G. Riveros, J.F. Guillemoles, M. Froment, Electrochem. Solid-State Lett. 7 (2004) C75–C77.
[18] A. Petrauskas, L. Grincevičienė, A. Češūnienė, R. Juškėnas, Electrochim. Acta 51 (2006) 4204–4209.
[19] A. Survilienė, P. Kalinauskas, A. Survilienė, A. Sudavičius, Chemija 18 (2007) 18–22.
[20] C. Kaito, A. Nonaka, S. Kimura, N. Suzuki, Y. Saito, J. Cryst. Growth 186 (1998) 386–392.
[21] A. Lukinskas, V. Jasulaitienė, P. Lukinskas, I. Savickaja, P. Kalinauskas, Electrochim. Acta 51 (2006) 6171–6178.